Mineral dust intrusions in Southeastern Romania: insights from seventeen years of sun photometer data

G. CIOCAN[1,2], A. NEMUC[1,*], L. BELEGANTE[1], M. M. CAZACU[3,4]
[1]*National Institute of Research and Development for Optoelectronics INOE 2000, Magurele, 077125, Romania*
[2]*Faculty of Physics, University of Bucharest, Magurele, 077125, Romania*
[3]*Department of Physics, "Gheorghe Asachi" Technical University of Iasi, 700050 Iaşi, Romania*
[4]*INOESY SRL, 8 Fdc. Mestecanis Street, 707410, Valea Lupului, Iasi, Romania*

Atmospheric mineral dust impacts climate, air quality, and cloud microphysics. This study analyzes 17 years (2007–2024) of dust intrusions over Southeast Romania using advanced optoelectronic instrumentation, specifically AERONET sun photometer data from RADO-Bucharest. By applying aerosol optical depth and Ångström Exponent, we classify dust events by duration and intensity, revealing an annual increase of 1.08 dust days and 0.6 distinct events. Dust transport peaks in late spring, with May showing the highest occurrence. Composition shifts indicate increased marine and mixed aerosols. These findings highlight the growing influence of transported dust and the need for continued monitoring in evolving climate conditions.

(Received March 20, 2025; accepted August 5, 2025)

Keywords: Mineral dust, Dust event classification, Photometer data, Aerosol composition

1. Introduction

Optoelectronic technologies have become essential tools for investigating atmospheric aerosols, particularly mineral dust, which plays a critical role in influencing Earth's radiation balance, cloud microphysics, and precipitation dynamics. Mineral dust is notable for its widespread presence and capacity for long-range transport, impacting regions far from its source. The interaction of dust particles with solar radiation leads to both scattering and absorption effects, which modify the radiative budget of the atmosphere. Furthermore, dust acts as effective cloud condensation nuclei (CCN) and ice nucleating particles (INP), thereby influencing cloud formation and precipitation processes [1,2].

Research has established the dual role of dust as both a climatic driver and a pollutant. Studies by [3] have highlighted the intricate interplay between dust emissions, atmospheric chemistry, and radiative forcing. These studies emphasize that dust not only contributes to direct radiative forcing through its optical properties but also affects cloud properties and precipitation patterns, which are critical in the context of global climate change [4,5]. The significance of dust in modulating cloud properties and precipitation dynamics has been further supported by studies on aerosol-cloud interactions, such as those by [6] and [7], which underscore the importance of understanding these interactions in the face of changing aerosol loading and its potential feedback mechanisms on regional climate dynamics.

Recent studies have documented a significant intensification of Saharan dust transport toward Europe [8] identified a sharp increase in the frequency and magnitude of dust intrusions over the western Euro-Mediterranean during February–March 2020–2022, highlighting shifts in large-scale circulation patterns that favor enhanced dust mobilization and northward transport. Such findings indicate broader regional changes that may also influence Eastern and Southeastern Europe. Additionally, [9] reported a doubling of annual dust deposition events in Central Europe during the 2010s, further suggesting a trend of increasing dust activity across the continent. These regional-scale observations provide important context for the current study, which focuses on long-range dust transport reaching Southeastern Romania.

Despite the extensive body of research on dust-aerosol interactions, there remains a notable gap in studies focusing on regions affected by long-range dust transport in Romania, usually focused on case study events (e.g. [10-14]**)**. While dust research in the region is limited, extensive studies using the AERONET sun photometer in Romania have provided valuable insights into aerosol properties and atmospheric processes ([15-20]**)**. This site, lacking significant local dust sources, provides a unique opportunity to study the effects of long range transported dust events. The RADO-Bucharest observational site, strategically located in a flat landscape surrounded by agricultural and urban areas, is particularly well-suited for monitoring dust episodes originating from remote sources, especially the Saharan and Arabian deserts. The geographic setting of this site allows for the examination of complex atmospheric processes, including the mixing of transported dust with local pollutants and the alteration of aerosol properties during transport [21,22].

This study aims to conduct one of the first long-term analyses of mineral dust intrusions in Romania using ground-based remote sensing data from the AERONET network. While satellite observations provide broad spatial

coverage, they often lack the temporal resolution necessary for detailed analysis and can be affected by cloud contamination. AERONET data offers high-frequency measurements with stringent quality control, enabling a more precise assessment of dust events over the region [23,24]. By analyzing long-term trends in dust events from June 2007 to June 2024, this research will classify dust events based on duration and intensity, assess seasonal variations, investigate changes in aerosol composition during dust events, and explore the implications of increased dust activity for climate dynamics and air quality [25,26].

In conclusion, the study of mineral dust aerosols is essential for understanding their multifaceted roles in climate systems. The findings from this research will contribute to the broader understanding of dust's impact on atmospheric processes, particularly in regions influenced by long-range transport, thereby providing valuable insights into the implications of dust for climate dynamics and air quality.

2. Data and methodology

2.1. Data collection and instrumentation

The analysis presented in this study utilizes Level 2 (L2) quality-assured data from the AERONET sun photometer located at the RADO-Bucharest National Facility, as part of the ACTRIS (Aerosol, Clouds, and Trace Gases Research Infrastructure) pan-european infrastructure. The dataset spans from June 2007 to June 2024 and encompasses measurements across multiple spectral bands (340, 380, 440, 500, 670, 870, 940, and 1020 nm). This comprehensive dataset is instrumental in capturing aerosol optical properties, as the sun photometer records both direct solar irradiance and sky radiance, thereby providing a detailed understanding of aerosol dynamics under varying atmospheric conditions [20].

The AERONET sun photometer, an optoelectronic remote sensing system, is equipped with state-of-the-art interference filters that facilitate high spectral resolution, crucial for the precise spectral decomposition of incoming solar radiation. Its optoelectronic design enables reliable operation across a wide range of air mass conditions—from early morning to late evening—effectively capturing diurnal variations in aerosol concentrations. This functionality is further enhanced by multi-angular sky radiance measurements conducted in two scanning geometries: the solar almucantar and the principal plane. These scans provide critical data for retrieving aerosol microphysical properties via the Dubovik and King inversion algorithm [27].

In addition, the AERONET Level 2 data have undergone rigorous quality assurance procedures, including cloud screening using advanced symmetry checks and variability tests. Radiometric calibration, carried out periodically with reference spheres, ensures the stability of the instrument's measurements [28]. Furthermore, the dynamic characterization of surface albedo through satellite-derived data enhances the accuracy of aerosol retrievals, especially over heterogeneous surfaces. The integration of satellite-derived albedo products has been shown to significantly improve the retrieval of aerosol properties, particularly in regions with complex land cover [29,30]. These measures collectively result in a high-confidence dataset that is critical for long-term trend analysis.

2.2. Aerosol classification

AERONET data provides a comprehensive framework for classifying aerosols through cluster analysis, which investigates relationships among multiple parameters. The methodologies developed by [31] and [32] established aerosol type classifications using Aerosol Optical Depth (AOD) and the Ångström Exponent (AE), where AE < 0.5 and AOD > 0.15 typically indicates pure dust, and AE between 0.5–1.2 suggests dust mixed with pollution when AOD remains above 0.15. In this study, we applied a dust classification threshold of AE < 1.15 and AOD > 0.2, a range consistent with several aerosol studies in Romania and Eastern Europe [17,33].

However, this method has limitations—particularly in differentiating between absorbing and non-absorbing anthropogenic aerosols when geographic context is not considered. To overcome this, [34] proposed incorporating additional thresholds based on the Single Scattering Albedo (SSA) at 440 nm and the Fine Mode Fraction (FMF) at 550 nm. FMF provides a more quantitative assessment of particle size compared to the more qualitative Ångström Exponent. Subsequent improvements by [35] and [36]further integrated the Ångström Exponent with revised threshold values to enhance the classification of mixed aerosols.

For this study, we opted for the initial classification approach utilizing AOD and the Ångström Exponent (Fig 1), which effectively identifies dust-dominant events and distinguishes them from other aerosol types. This method not only facilitates robust detection of dust-laden air masses but also aligns with established classification methodologies, as supported by the findings of [37] and [38]**.** Another reason for choosing this method relates to data availability. The second method, which relies on parameters such as Single Scattering Albedo (SSA), Ångström Exponent (AE), and Fine Mode Fraction (FMF), requires more rigorous data screening. This significantly reduces the number of usable measurements—an important limitation for a study of this kind. Therefore, we opted for the first method, which allows us to include the maximum number of measurement days.

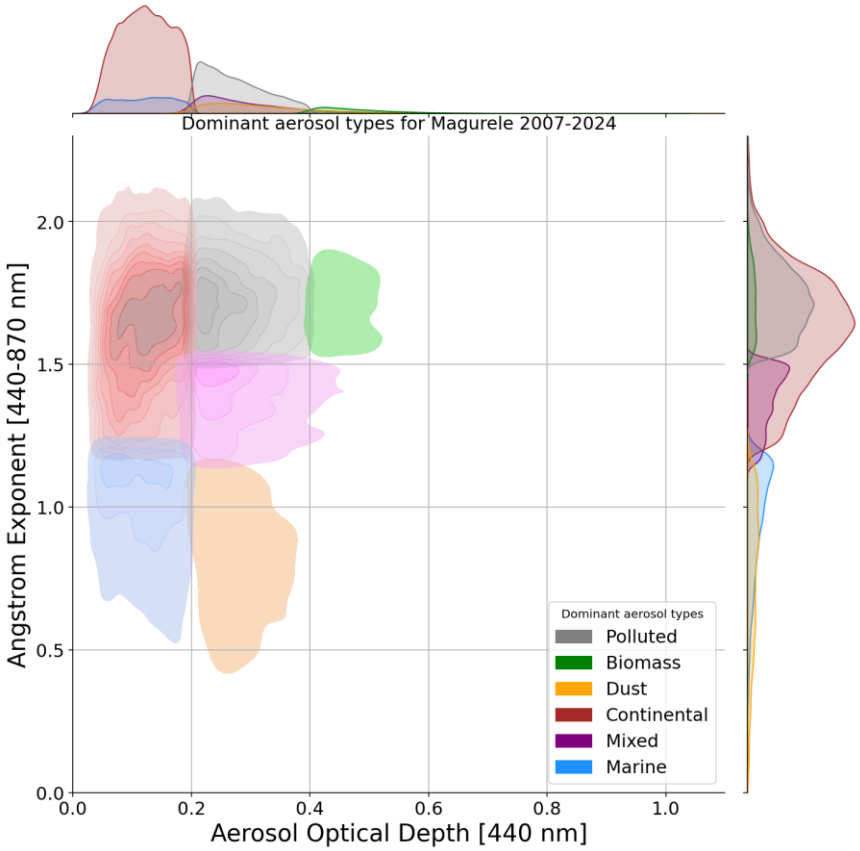

Fig. 1. Distribution of dominant aerosol types for Măgurele (2007–2024) based on the Ångström Exponent (440–870 nm) and Aerosol Optical Depth (440 nm). The classification follows the standard methodology discussed in the first part of section 2.2 without considering the twilight zones (colour online)

2.3. Dust event definition and classification

Threshold-based classification methods can be overly rigid, particularly near cluster boundaries, where the optical properties of aerosols may overlap due to atmospheric mixing. Instruments such as sun photometers often cannot sharply distinguish aerosol types in these transitional regions. To address this limitation, we employed Kernel Density Estimation (KDE) as a complementary technique. KDE allows visualization of the continuous distribution of AOD–AE values beyond fixed thresholds, providing a probabilistic understanding of aerosol populations and making it possible to identify and quantify mixing zones between different aerosol types—insight that binary classification schemes might overlook. This method allows for a nuanced understanding of aerosol distributions and their temporal characteristics, which is essential for effective monitoring and classification of dust events [39,40]. We establish threshold criteria that delineate dust events into the following categories:

- Duration:
  - Long: Events lasting more than 5 consecutive days.
  - Medium: Events lasting between 2 and 5 days.
  - Short: Events lasting less than 2 days.
- Intensity:
  - Strong: Events where at least 80% of the aerosol points measured are classified as dust.
  - Weak: Events with less than 80% of aerosol points measured being classified as dust.

The classification of dust events based on duration and intensity is supported by findings that highlight the significance of both parameters in understanding the impact of dust on air quality and climate [41,42].

2.4. Kernel density estimation for twilight zones

An important aspect of our methodology is the identification of overlapping aerosol types, commonly referred to as the "twilight zones." This process involves several steps:

- **Step 1:** Understanding KDE

For each aerosol type, we extract AOD and AE values and apply the Gaussian KDE to estimate a continuous probability density function (PDF) over the AOD-AE space. Higher density values indicate regions with a greater concentration of data points.

- **Step 2**: Computing KDE for Two Aerosol Types

To determine the overlap between "Dust" and "Continental" aerosols, for example, we compute their respective KDEs over a defined grid covering the AOD-AE space.

- **Step 3**: Finding the Intersection

We calculate the intersection density (ID) at each grid point using:

$$ID\ (x,y) = \min(PDF_{dust}(x,y), PDF_{marine}(x,y)) \quad (1)$$

This approach ensures that regions where both aerosol types have high density are emphasized.

- **Step 4**: Thresholding the Intersection

To avoid including areas with negligible overlap, we define a threshold as 10% of the maximum intersection density:

$$Threshold = 0.1 \times Intersection\ Density \quad (2)$$

We then create a binary mask: grid points with intersection density greater than this threshold are considered part of the twilight zone.

- **Step 5:** Extracting Data Points

Finally, each data point in the dataset is mapped to the closest grid point. If the corresponding grid location falls within the intersection mask, that data point is classified as part of the twilight zone. These points are subsequently highlighted on the KDE plot (Fig 2), visually representing the overlap between aerosol types.

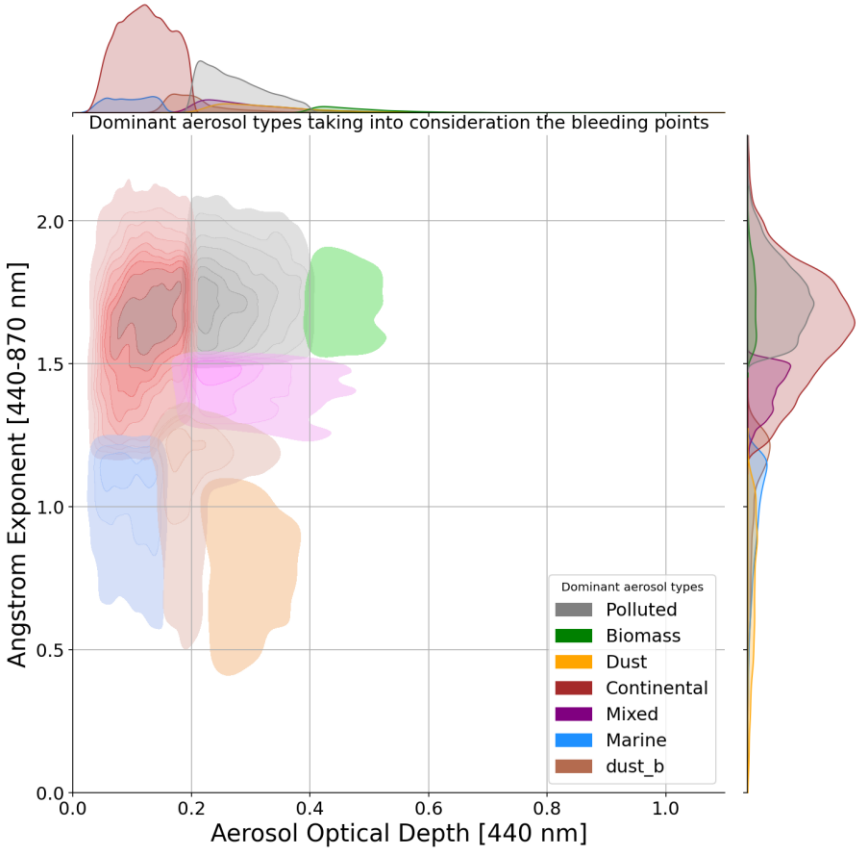

Fig. 2. Aerosol classification diagram incorporating the "twilight zone" concept. The term bleeding points, as referenced in the figure title, denotes data points located within the twilight zone—regions where aerosol types overlap. This terminology applies to all types of twilight zones, not only those involving dust. The dust_b label in the legend refers specifically to points within the dust-related twilight zone, representing a mixture of dust and other aerosol types—hence the name. The figure uses Kernel Density Estimation (KDE) to visualize the overlap and distribution of different aerosol categories) (colour online)

2.5. Dust day calculation based on seasonal daylight

In addition to aerosol classification, we determine "dust days" by considering the number of dust points in relation to the available daylight. The dataset is divided into two distinct seasons:

- Cold Season: January 1–March 21 and October 23–December 31
- Warm Season: March 22–October 22

During the warm season, days typically feature more than 12 hours of daylight, with sunrise before 07:00 and sunset after 19:00.

For each season, we compute the average number of valid measurement points per day.

A day is defined as a "dust day" if it records at least half of the average number of valid measurement points as dust points (dust or dust_b). This threshold ensures that only days with a significant presence of dust, as reflected by the frequency of measurements, are classified as dust days. A comprehensive visualization method is presented in Fig. 3.

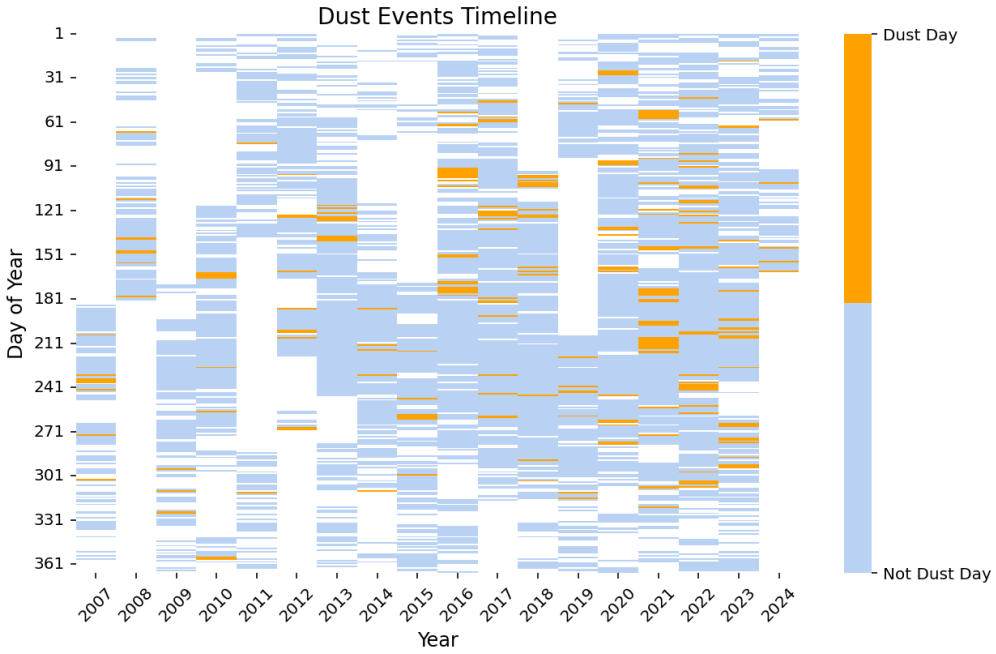

Fig. 3. Temporal distribution of dust events from 2007 to 2024. Each row represents a day of the year, with dust days marked in orange and non-dust days in blue. Gaps indicate missing or unavailable data (colour online)

3. Results

3.1. Long-term trends in dust events

Our analysis reveals a clear upward trend in dust events over the study period. On average, the number of dust days increased by approximately 1.08 days per year (Fig. 4), while the frequency of distinct dust events grew by about 0.6 events annually (Fig. 5). This increasing trend is statistically significant ($p < 0.05$) and underscores a progressive rise in dust activity in the region.

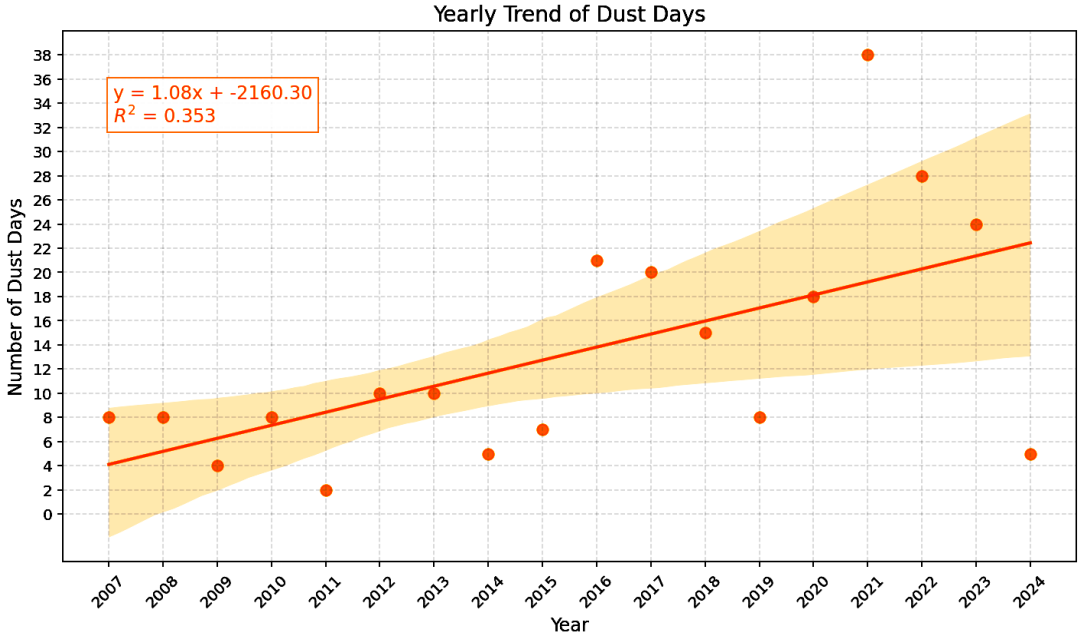

Fig. 4. Scatter plot of annual dust days from 2007 to 2024, showing individual data points and a regression trend line. The shaded area represents the confidence interval of the trend (colour online)

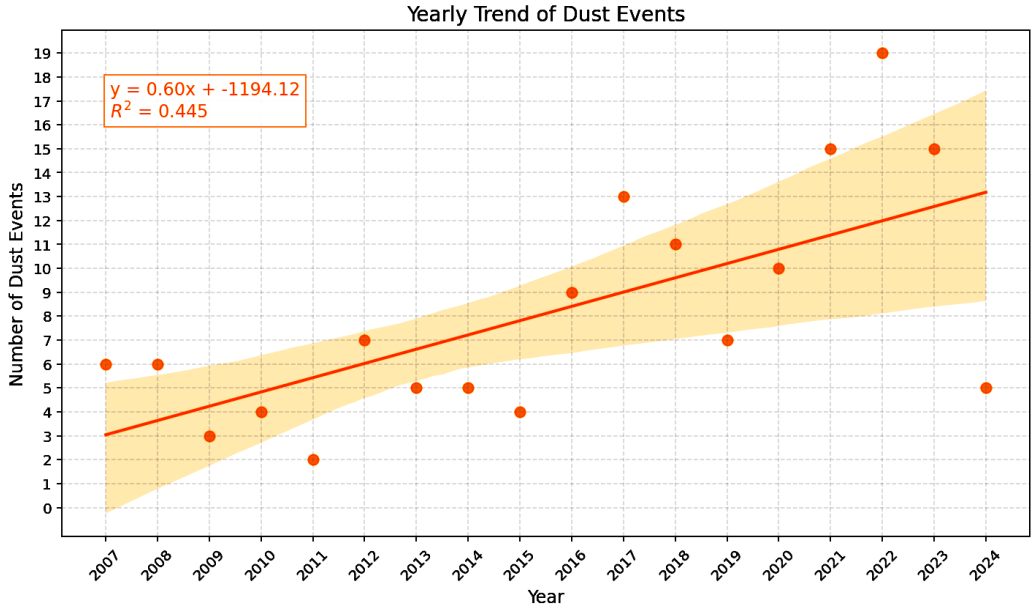

Fig. 5. Scatter plot of annual distinct dust events from 2007 to 2024, with individual data points, a regression trend line, and a shaded confidence interval (colour online)

A seasonal breakdown indicates that dust events have become more frequent in both warm and cold seasons (Fig. 6), though the increase is more pronounced in the warm season, with a slope of 0.29 events per year, compared to 0.18 events per year in the cold season. This seasonal disparity suggests that higher ambient temperatures and enhanced wind speeds during warmer months contribute to increased dust mobilization and transport [43]. The relationship between temperature and dust events is well-documented, as warmer conditions often lead to drier soil, which is more susceptible to erosion and dust lifting [43,44]. Furthermore, the influence of wind speed on dust emissions is important, as increased wind can exacerbate dust transport, particularly in arid and semi-arid regions [43].

Another factor influencing this seasonal difference is the higher number of measurements conducted during the warm season. Since sun photometers rely on clear-sky conditions for data collection, they are more likely to record dust events in spring and summer when cloud cover is minimal. This observational bias may partially explain the stronger trend observed in warm-season dust activity.

Additionally, studies have indicated that the frequency of dust events can be significantly affected by human activities and land use changes, which can alter the natural dust emission sources [45].

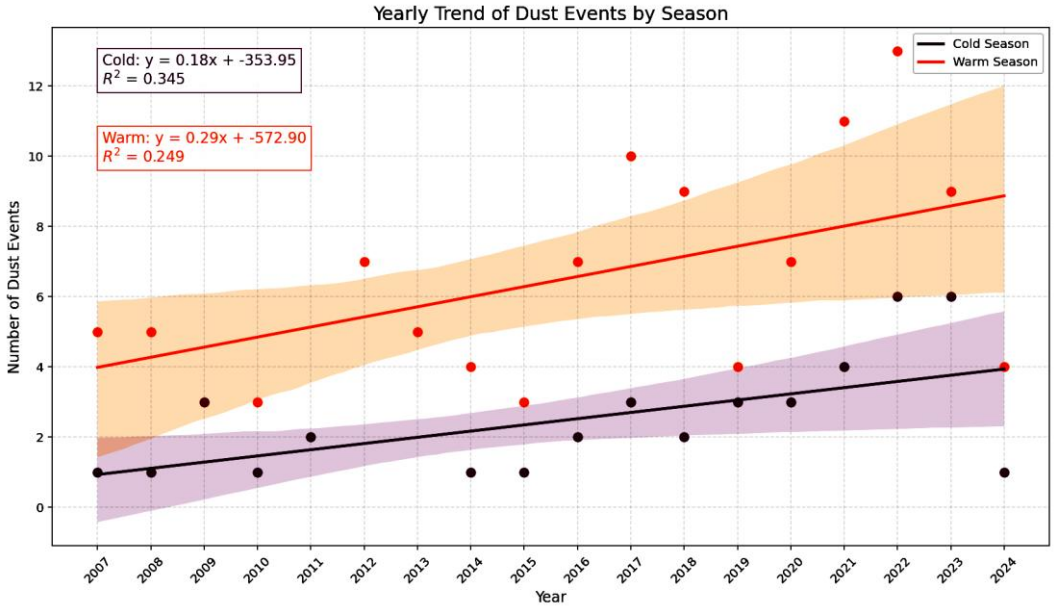

Fig. 6. Scatter plot of annual dust events for the cold and warm seasons from 2007 to 2024. Orange and purple regression trend lines represent the seasonal variations in dust event frequency (colour online)

3.2. Seasonal and monthly variations

A robust seasonal cycle is evident in the occurrence of dust events (Fig. 7), with May consistently experiencing the highest frequency of such events, followed by June. This pattern indicates that late spring and early summer are the most active periods for dust transport in the region. The peak in dust events during these months coincides with increased atmospheric instability and enhanced long-range transport conditions [46-48].

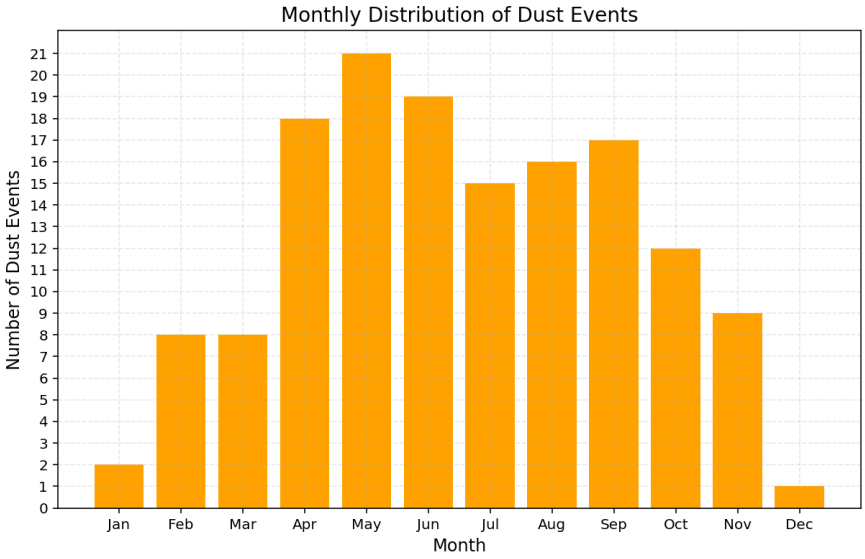

Fig. 7. Monthly histogram of dust event occurrences from 2007 to 2024. The bars represent the total number of dust events recorded each month (colour online)

Intensity-based analysis (Fig. 8) reveals that weak-intensity dust events dominate the seasonal distribution, peaking in May and maintaining activity through the summer months. In contrast, strong-intensity events show a more gradual increase from April through September, suggesting that severe dust intrusions are not confined to a single peak month but are instead distributed over an extended warm-season period. This trend may be associated with changes in synoptic-scale circulation patterns that facilitate dust outbreaks from various source regions at different times of the year [35,49]. The variability in dust event intensity can be attributed to the interplay between local meteorological conditions and broader climatic phenomena, such as El Niño and La Niña, which affect wind patterns and moisture availability [46,50]

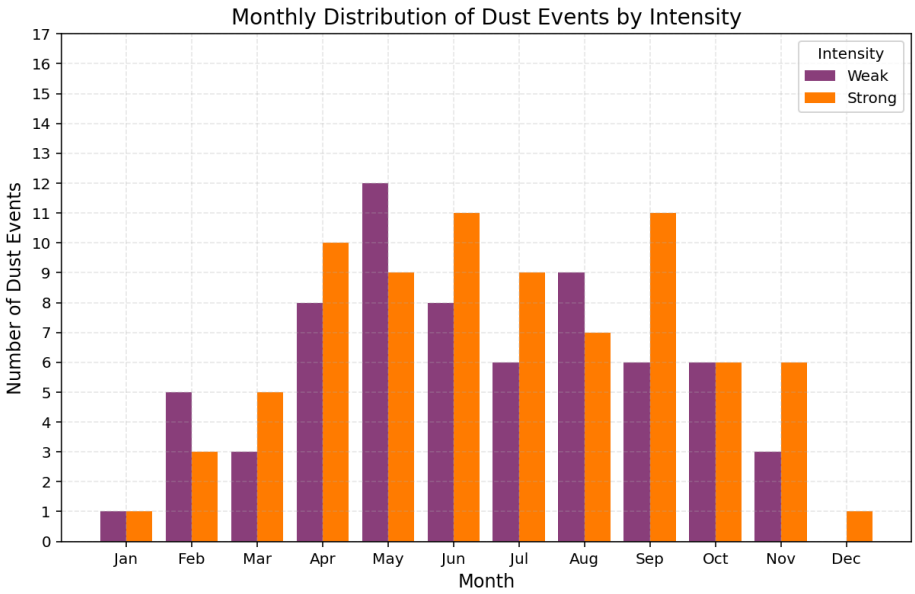

Fig. 8. Monthly histogram of dust events classified by intensity. Bars are divided into strong and weak dust events based on the percentage of dust mass composition (colour online)

A detailed breakdown of dust event durations (Fig. 9) provides further insights into the nature of these occurrences. Short-duration events are relatively frequent throughout the year but show a pronounced increase from April to September, with a peak in May. This suggests that while dust outbreaks occur year-round, transient dust intrusions are more common during periods of increased regional dust transport [51]. Medium-duration events are most frequent in May, aligning with periods of enhanced meteorological instability and lower soil moisture levels, which favor both dust mobilization from source regions and the maintenance of dust-laden air masses over the region [52,53]. Long-duration events, though less common, exhibit a gradual increase in frequency during the warmer months, indicating the influence of sustained atmospheric circulation patterns that allow dust to remain suspended for extended periods, particularly in stable summer conditions [54,55].

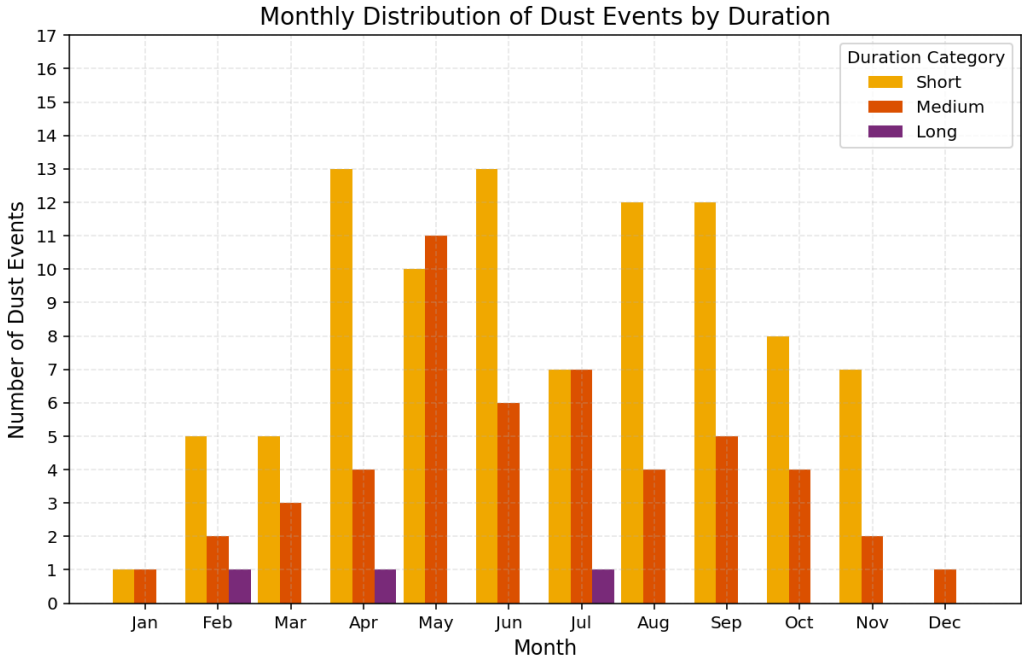

Fig. 9. Monthly histogram of dust events classified by duration. The bars represent short, medium, and long-duration dust events over the study period (colour online)

3.3. Variations in dust event characteristics

Short-duration dust events have exhibited the most significant increase in frequency, aligning with the overall trend of more frequent dust occurrences (Fig. 10). With a slope of 0.34 events per year, these events show a clear upward trajectory, suggesting that dust outbreaks are becoming more frequent but not necessarily prolonged. This trend is supported by findings from [56], who noted that large-scale atmospheric circulation anomalies significantly influence dust transport, thereby contributing to the increased frequency of such events. Medium-duration dust events have also increased, albeit at a slightly lower rate (0.24 events per year), indicating that conditions conducive to dust transport and suspension persist for longer periods. This persistence can be attributed to long-term changes in atmospheric circulation patterns, which have been linked to increased aridity in various regions, as highlighted by [57]**.** While long-duration dust events remain relatively rare, their gradual increase (0.02 events per year) suggests that shifts in atmospheric circulation patterns may be favoring prolonged dust transport in certain cases, a phenomenon that has been documented in multiple studies [57,58].

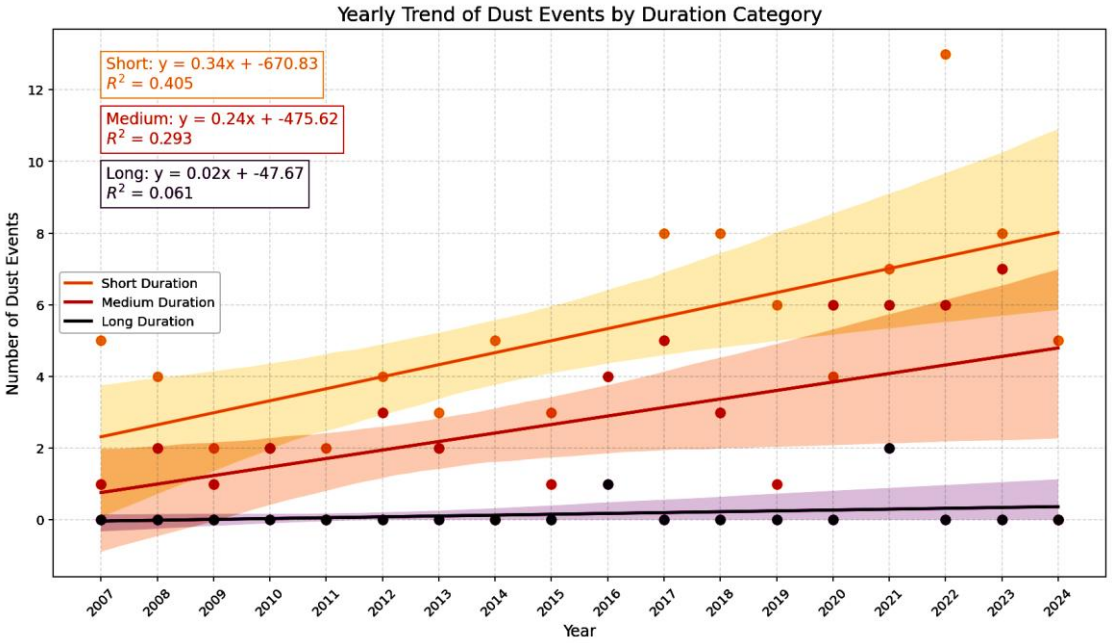

Fig. 10. Yearly trend of dust event durations from 2007 to 2024. The figure categorizes events by short, medium, and long duration, showing their respective trends (colour online)

The intensity of dust events follows a similar increasing trend (Fig. 11). Weak-intensity dust events have shown the steepest rise (0.37 events per year), suggesting a greater prevalence of low-concentration dust intrusions. This could be attributed to increased dust mobilization from distant sources, likely facilitated by changing wind patterns and regional meteorological conditions, as discussed by [59]. Strong-intensity dust events, while increasing at a slower rate (0.23 events per year), still demonstrate a clear upward trend, reinforcing the notion that both frequency and severity of dust transport episodes are on the rise. The simultaneous growth in both weak and strong intensity categories suggests an overall increase in dust load reaching the region. This dual increase in intensity categories indicates a complex interplay between local and regional climatic factors that govern dust dynamics.

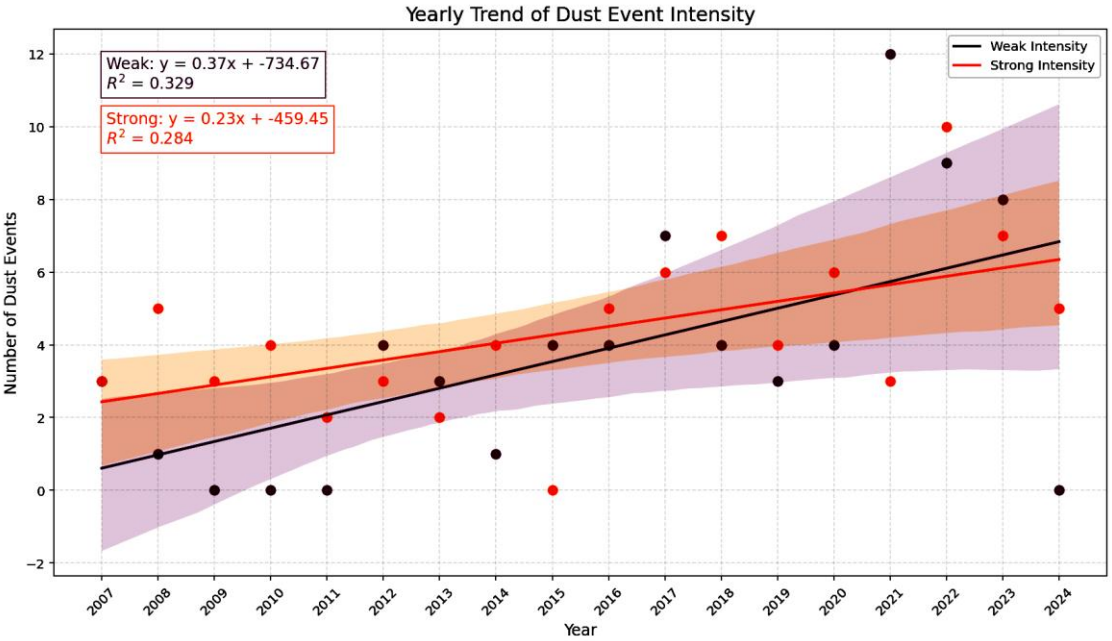

Fig. 11. Yearly trend of dust event intensities from 2007 to 2024. The plot distinguishes between strong and weak intensity events over time (colour online)

3.4. Aerosol type composition and trends

An analysis of aerosol types within dust events (Fig. 12) indicates that marine aerosols have experienced a substantial increase, suggesting a stronger interaction between dust transport and maritime air masses over time. This increase can be attributed to changes in atmospheric circulation patterns that facilitate the mixing of dust with humid air from marine environments, potentially altering dust optical and microphysical properties. Studies have shown that the mixing of mineral dust with urban pollution can significantly impact the radiative properties of aerosols, enhancing their effects on climate [60].

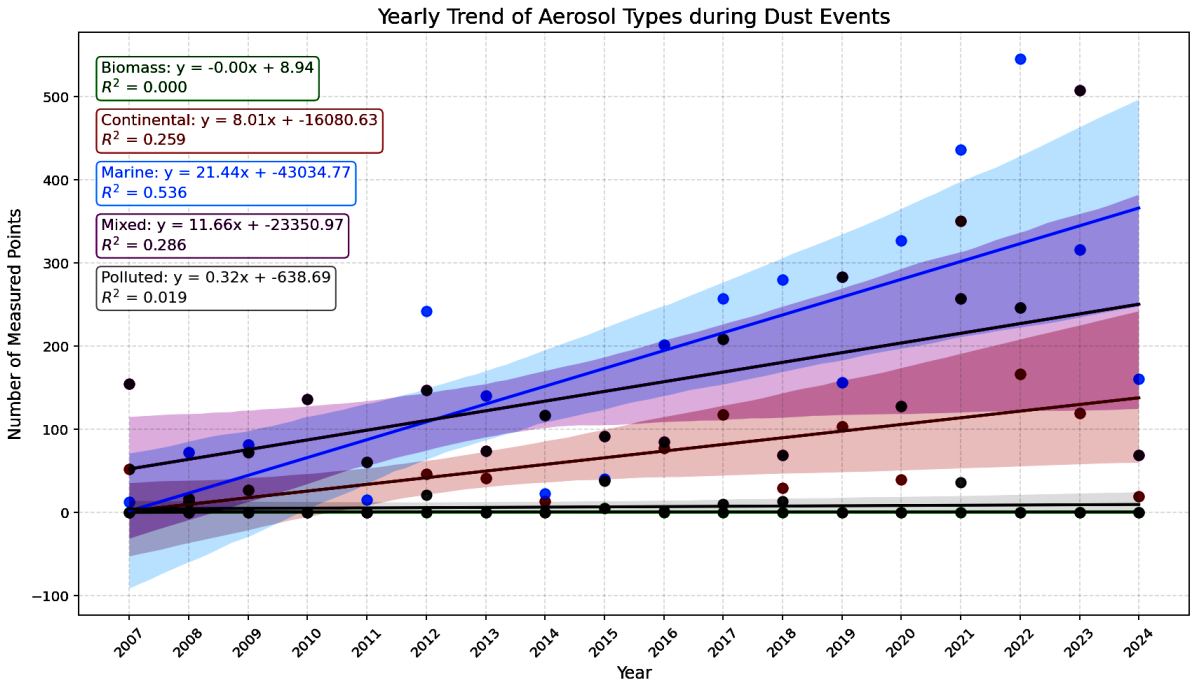

Fig. 12. Yearly trend of aerosol type distributions during dust events. The figure shows the relative contributions of different aerosol types, including dust, marine, continental, mixed, biomass and polluted aerosols (colour online)

Continental aerosols have also shown a notable increase, reflecting broader shifts in regional aerosol composition. This rise may be associated with increased resuspension of local soil dust or anthropogenic influences, such as land use changes and industrial activities, which contribute to the background aerosol load during dust events. Research indicates that anthropogenic aerosols can significantly alter the composition and properties of natural aerosols, leading to enhanced interactions during dust intrusions [61]. Similarly, mixed aerosols have increased, indicating enhanced interactions between different aerosol types during dust intrusions, likely due to long-range transport and mixing with locally emitted particles.

Polluted aerosols, while exhibiting only a slight upward trend, suggest that anthropogenic contributions to atmospheric particulates remain a factor in modifying dust properties. This could be linked to urban emissions or secondary aerosol formation, which may influence the optical and hygroscopic characteristics of transported dust. The interaction between anthropogenic and natural aerosols has been shown to enhance the formation of secondary organic aerosols, which can further complicate the atmospheric chemistry during dust events [62]. Moreover, the role of urban pollution in altering the physical and chemical properties of aerosols has been well documented, indicating that even minor increases in polluted aerosols can have significant implications for air quality and climate [63].

Biomass-burning aerosols appear to be absent during dust events in our dataset; however, this absence is most likely a result of methodological bias rather than a true lack of interaction. The classification approach used relies on strict threshold-based criteria, which may overlook mixed aerosol conditions—particularly in transitional zones where properties overlap. While it is true that in some cases, biomass-burning and dust events do not coincide due to differing transport pathways or source region timing, such cases are relatively rare. Given the 2007–2024 timeframe, it is improbable that no overlap occurred at all. Previous long-term studies have shown that interactions between dust and biomass-burning aerosols are not uncommon, although their detection depends heavily on the classification method and the resolution of available measurements [64], [65]. Therefore, the lack of biomass-burning signatures during dust episodes in this study should be interpreted cautiously and understood primarily as a limitation of the method.

The classification approach underscores a significant separation in the occurrence of biomass-burning and dust aerosols, particularly during dust events. This delineation is valid within the dataset examined and reflects specific contextual attributes of the study without generalizing interactions in other regions or under varying atmospheric conditions.

4. Discussion

4.1. Implications for climate and air quality

The increasing frequency and intensity of dust events have significant implications for both regional climate and air quality. Enhanced dust loading can lead to alterations in the Earth's radiative balance, either by direct scattering and absorption of solar radiation or indirectly through modifications to cloud microphysics. Studies indicate that dust particles interact with other aerosol types, such as marine and mixed aerosols, which can alter their optical properties and consequently their climatic impacts ([24,66,67]. The direct radiative effects of dust aerosols are substantial, contributing approximately 30% to the total aerosol global mean direct radiative effect [68]. This interaction is critical as it can influence cloud formation and precipitation patterns, thereby affecting regional climate systems [69,70, p. 21]

In urban and industrial regions, the mixing of dust with anthropogenic pollutants exacerbates air quality issues, leading to higher concentrations of fine particulate matter (PM2.5) and potential public health risks [71]. The integration of dust event data into climate models and air quality forecasting systems is essential for accurately predicting future environmental conditions and understanding the health implications associated with increased particulate matter exposure [24,72].

4.2. Limitations and uncertainties

While our analysis is based on a high-quality AERONET dataset, several limitations must be acknowledged. The spatial coverage of ground-based observations is inherently limited, which restricts the generalizability of our results to broader regional or global scales.

Although our classification scheme effectively distinguishes dust-dominated events, uncertainties remain regarding the contributions of mixed aerosol sources, particularly in regions influenced by both natural and anthropogenic emissions [73].

Another key limitation stems from the instrumental constraints of the sun photometer itself. AERONET measurements rely on direct sunlight, meaning data acquisition is disrupted on cloudy or rainy days, resulting in observational gaps. This is particularly relevant during dust events occurring under mixed meteorological conditions, where interactions between dust and clouds may affect aerosol properties but remain underrepresented in the dataset. Additionally, data availability is influenced by periodic calibration intervals, during which instruments are offline, further reducing temporal coverage. This issue is more pronounced in earlier years of the study period, when fewer measurement days were recorded. As a result, there is a bias in data density across the 2007–2024 interval, with a greater number of observations available in more recent years. This could potentially influence the slope of long-term trends, particularly in regions where increasing aerosol activity is observed. Nevertheless, because the positive slope of these trends is generally consistent with the more densely sampled recent period, we consider the missing data unlikely to significantly alter the main findings of the study.

Future studies could mitigate these uncertainties by integrating AERONET data with satellite-based observations and ground-based lidar measurements, improving both the vertical and horizontal resolution of dust detection [35,74]. Advancements in retrieval algorithms and enhanced calibration protocols could further reduce measurement uncertainties, particularly in mixed aerosol environments [21].

4.3. Future research directions

Future research will extend the current work by investigating detailed dust source regions and transport mechanisms, with particular focus on the role of land use changes and anthropogenic influences. Additionally, future efforts will aim to refine the classification methodology itself, improving sensitivity to mixed aerosol types and reducing biases introduced by threshold-based approaches.

Developing advanced modeling techniques that integrate AERONET data with satellite and lidar observations will allow for more accurate simulations of the radiative effects of dust aerosols.

Additionally, expanding analyses of dust–cloud interactions, with a special emphasis on assessing changes in cloud properties, will be crucial. By incorporating lidar data, future studies will better profile the vertical distribution of dust and its influence on cloud formation, microphysical properties, and precipitation patterns.

Conducting longitudinal studies to evaluate how evolving climatic conditions—such as rising temperatures and altered wind patterns—affect dust event frequency, duration, and intensity will also be essential for understanding the broader climatic and environmental impacts of dust.

5. Conclusion

This comprehensive study, grounded in optoelectronic remote sensing techniques, documents significant long-term trends in dust events over a 17-year period using AERONET sun photometer data. Our results indicate a statistically significant increase in both the number of dust days and distinct dust events, with pronounced seasonal and compositional variations. The upward trend is most evident during the warm season, emphasizing the

influence of climatic factors such as temperature and wind speed on dust mobilization. Previous research has similarly identified positive linear trends in dust event frequency, particularly in regions like the northern Great Plains and the southwestern U.S., which aligns with our findings regarding seasonal variations and the impact of climatic conditions on dust emissions [59,75].

The detailed methodology, including the KDE-based calculation of twilight zones and the seasonal dust day, enhances our understanding of aerosol interactions and the impact of daylight availability on data collection.

The observed shift in aerosol composition, notably the increase in marine and mixed aerosols, suggests that the interplay between natural dust and anthropogenic emissions is becoming more complex. This complexity is supported by findings that demonstrate how variations in local surface conditions, such as soil moisture and vegetation, significantly influence dust emissions and transport [75,76].

Moreover, the implications for radiative forcing and cloud dynamics are critical, as changes in aerosol composition can affect cloud properties and atmospheric profiles, which has been documented in various studies [77,78].

Future work, particularly the integration of lidar and other remote sensing techniques, will be essential for assessing how dust events influence cloud properties and atmospheric profiles. The use of advanced remote sensing technologies has already provided valuable insights into the vertical distribution and transport pathways of dust aerosols, highlighting the need for comprehensive monitoring systems to understand the dynamics of dust events better [79,80]. Furthermore, the seasonal variability of dust transport, particularly in relation to climatic factors, underscores the importance of continued research in this area to develop predictive models for dust activity [81].

Acknowledgements

This work was carried out through the Core Program within the National Research Development and Innovation Plan 2022-2027, with the support of MCID, project no. PN23 05/ 3.01.2023 and was financed by Smart Growth, Digitization and Financial Instruments Program (PoCIDIF) 2021-2027, Action 1.3 Integration of the national RDI ecosystem in the European and international Research Space, project "Supporting the operation of facilities in Romania within the ACTRIS ERIC research infrastructure", SMIS code 309113.

The research was partially funded by the European Regional Development Fund through the Competitiveness Operational Programme 2014-2020, POC-A.1-A.1.1.1- F-2015, project Research Centre for Environment and Earth Observation CEO-Terra, SMIS code 108109, contract No.152/2016.

Authors acknowledge AERONET-Europe for providing calibration service. AERONET-Europe is part of ACTRIS Research Infrastructure.

References

[1] B. Heinold, J. Helmert, O. Hellmuth, R. Wolke, A. Ansmann, B. Marticorena, B. Laurent, I. Tegen, Journal of Geophysical Research Atmospheres **112**, D11204 (2007).
[2] V. A. Karydis, P. Kumar, D. Barahona, I. N. Sokolik, A. Nenes, J. Geophys. Res. **116**, D23204 (2011).
[3] N. Mahowald, S. Albani, J. Kok, S. Engelstaeder, R. Scanza, D. Ward, M. Flanner, Aeolian Research **15**, 53 (2014)
[4] P. Knippertz, M. C. Todd, Reviews of Geophysics **50**(1), 2011RG000362 (2012).
[5] C. S. Zender, E. Y. Kwon, Journal of Geophysical Research Atmospheres **110**, D13201 (2005).
[6] W. Wang, J. Huang, P. Minnis, Y. Hu, J. Li, Z. Huang, J. Kirk Ayers, Tianhe Wang, Journal of Geophysical Research Atmospheres **115**, D00H35 (2010).
[7] B. Heinold, I. Tegen, E3s Web of Conferences **99**, 02012 (2019).
[8] E. Cuevas-Agulló, D. Barriopedro, R. D. García, S. Alonso-Pérez, J. J. González-Alemán, E. Werner, D. Suárez, J. J. Bustos, G. García-Castrillo, O. García, Á. Barreto, S. Basart, Atmos. Chem. Phys. **24**(7), 4083 (2024).
[9] G. Varga, O. Meinander, Á. Rostási, P. Dagsson-Waldhauserova, A. Csávics, F. Gresina, Environment International, **180**, 108243 (2023).
[10] D. C. Bostan, I. M. Miclăuș, C. Apetroaie, M. Voiculescu, A. Timofte, M. M. Cazacu, Atmosphere **14**, 1366 (2023).
[11] D. Nicolae, C. Talianu, J. Ciuciu, M. Ciobanu, V. Babin, J. Optoelectron. Adv. M. **8**(1), 238 (2006).
[12] B. Livio, C. Talianu, A. Nemuc, V. Nicolae, G. Ciocan, F. Toanca, O. G. Tudose, C. Radu, D. Nicolae, J. Optoelectron. Adv. M. **26**(9-10), 422 (2024).
[13] V. Nicolae, L. Belegante, J. Vasilescu, A. Nemuc, F. Toanca, O. G. Tudose, C. Radu, D. Nicolae, J. Optoelectron. Adv. M. **25**(3-4), 176 (2023).
[14] E. Carstea, K. Fragkos, Optoelectron. Adv. Mat. **18**(11-12), 562 (2024).
[15] D. Nicolae, A. Nemuc, L. Belegante, paper presented at the Remote Sensing, U. N. Singh and G. Pappalardo, Eds., Toulouse, France, 78320N (2010).
[16] M. M. Cazacu, A. Timofte, F. Unga, B. Albina, S. Gurlui, Journal of Quantitative Spectroscopy and Radiative Transfer **153**, 57 (2015).
[17] S. Stefan, S. Voinea, G. Iorga, Atmospheric Pollution Research **11**(7), 1165 (2020).
[18] A. Nemuc, I. Binietoglou, S. Andrei, A. Dandocsi, H. Stefanie, EPJ Web of Conferences **119**, 24001 (2016).
[19] E. Carstea, K. Fragkos, N. Siomos, B. Antonescu, L. Belegante, Theor Appl Climatol. **137**(3-4), 3149 (2019).
[20] H. I. Ștefănie, A. Radovici, A. Mereuță, V. Arghiuș, H. Cămărășan, D. Costin, C. Botezan, C. Gînscă,

N. Ajtai, Remote Sensing **15**(12), 3072 (2023).
[21] X. Yue, H. Liao, H. J. Wang, S. L. Li, J. Tang, Atmos. Chem. Phys. Discuss. **11**, 1121 (2011).
[22] Z. Huang, J. Huang, T. Hayasaka, S. Wang, T. Zhou, H. Jin, Environmental Research Letters **10**(11), 114018 (2015).
[23] J. Haywood, P. Francis, S. Osborne, M. Glew, N. Loeb, E. Highwood, D. Tanre, G. Myhre, P. Formenti, E. Hirst, Journal of Geophysical Research Atmospheres **108**(D18), 8577 (2003).
[24] J. Huang, P. Minnis, H. Yan, Y. Yi, B. Chen, L. Zhang, J. K. Ayers, Atmos. Chem. Phys. **10**(14), 6863 (2010).
[25] R. L. Miller, J. P. Perlwitz, I. Tegen, Journal of Geophysical Research Atmospheres **109**, D24209 (2004).
[26] J. M. Creamean, J. R. Spackman, S. Davis, A. B. White, Journal of Geophysical Research Atmospheres **119**(12), 12171 (2014).
[27] O. Dubovik, M. D. King, J. Geophys. Res. **105**(D16), 20673 (2000).
[28] B. N. Holben, T. F Eck, I. Slutsker, A. Smirnov, A. Sinyukc, J. Schafer, D. Giles, O. Dubovik, paper presented at the Asia-Pacific Remote Sensing Symposium, S.-C. Tsay, T. Nakajima, R. P. Singh and R. Sridharan, Eds., Goa, India, 64080Q (2006).
[29] D. Carrer, S. Moparthy, G. Lellouch, X. Ceamanos, F. Pinault, S. C. Freitas, I. F. Trigo, Remote Sensing **10**(8), 1262 (2018).
[30] J. Cedilnik, D. Carrer, J. Mahfouf, J. Roujean, Journal of Applied Meteorology and Climatology **51**(10), 1835 (2012).
[31] O. Dubovik, B. Holben, T. F. Eck, A. Smirnov, Y. J. Kaufman, M. D. King, D. Tanré, I. Slutsker, J. Atmos. Sci. **59**(3), 590 (2002).
[32] C. Toledano, V. E. Cachorro, A. Berjon, A. M. de Frutos, M. Sorribas, B. A. de la Morena, P. Goloub, Quart. J. Royal Meteoro. Soc. **133**(624), 624 (2007).
[33] S. Garofalide, C. Postolachi, A. Cocean, G. Cocean, I. Motrescu, I. Cocean, B. S. Munteanu, M. Prelipceanu, S. Gurlui, L. Leontie, Atmosphere **13**(3), 493 (2022).
[34] J. Lee, J. Kim, C. H. Song, S. B. Kim, Y. Chun, B. H. Sohn, B. Holben, Atmospheric Environment **44**(26), 3110 (2010).
[35] M. Zhang, Y. Ma, W. Gong, B. Liu, Y. Shi, Z. Chen, Atmospheric Environment **182**, 275 (2018).
[36] S.-A. Logothetis, V. Salamalikis, A. Kazantzidis, Atmospheric Research **250**, 105343 (2021).
[37] P. Sivaprasad, C. A. Babu, Meteorological Applications **21**(2), 241 (2012).
[38] S. Kinne, D. O'Donnel, P. Stier, S. Kloster, K. Zhang, H. Schmidt, S. Rast, M. Giorgetta, T. F. Eck, B. Stevens, Journal of Advances in Modeling Earth Systems **5**(4), 704 (2013).
[39] F. Höpner, F. A. Bender, A. M. L. Ekman, A. Andersson, Ö. Gustafsson, C. Leck, Journal of Geophysical Research Atmospheres **124**(15), 8743 (2019).
[40] A. Valenzuela, F. J. Olmo, H. Lyamani, M. Antón, A. Quirantes, L. Alados-Arboledas, Journal of Geophysical Research Atmospheres **117**, D06214 (2012).
[41] M. Ealo, A. Alastuey, A. Ripoll, N. Pérez, M. Cruz Minguillón, X. Querol, M. Pandolfi, Atmospheric Chemistry and Physics **16**(19), 12567 (2016).
[42] R. Tao, H. Che, Q. Chen, J. Tao, Y. Wang, J. Sun, H. Wang, X. Zhang, Aerosol and Air Quality Research **14**(3), 905 (2014).
[43] J. Csavina, J. P. Field, O. Félix, A. Y. Corral-Avitia, A. E. Sáez, E. A. Betterton, The Science of the Total Environment **487**, 82 (2014).
[44] F. Karagulian, M. Temimi, D. Ghebreyesus, M. Weston, N. K. Kondapalli, V. K. Valappil, A. Aldababesh, A. Lyapustin, N. Chaouch, F. Al Hammadi, A. Al Abdooli, Air Quality Atmosphere and Health **12**(4), 453 (2019).
[45] H. Pi, B. Sharratt, J. Lei, Journal of Geophysical Research Atmospheres **122**(12), 6652 (2017).
[46] H. Lee, Y. Honda, Y.-H. Lim, Y. L. Guo, M. Hashizume, H. Kim, Atmospheric Environment **89**, 309 (2014).
[47] L. Chen, M. Zhang, J. Zhu, A. Skorokhod, Atmospheric Research **187**, 42 (2017).
[48] P. Ginoux, J. M. Prospero, T. E. Gill, N. C. Hsu, M. Zhao, Reviews of Geophysics **50**(3), 2012RG000388 (2012).
[49] K. T. Kanatani, I. Ito, W. K. Al-Delaimy, Y. Adachi, W. C. Mathews, J. W. Ramsdell, Am. J. Respir. Crit. Care Med. **182**(12), 1475 (2010).
[50] J. Guo, H. Liu, Z. Li, D. Rosenfeld, M. Jiang, W. Xu, J. H. Jiang, J. He, D. Chen, M. Min, P. Zhai, Atmos. Chem. Phys. **18**(18), 13329 (2018).
[51] K. Ardon-Dryer, M. C. Kelley, X. Xueting, Y. Dryer, Atmos. Meas. Tech. **15**(8), 2345 (2022).
[52] M. Notaro, Y. Yu, O. V. Kalashnikova, Journal of Geophysical Research Atmospheres **120**(19), 10229 (2015).
[53] G. Bergametti, B. Marticorena, J. L. Rajot, B. Chatenet, A. Féron, C. Gaimoz, G. Siour, M. Coulibaly, I. Koné, A. Maman, A. Zakou, Journal of Geophysical Research Atmospheres **122**(22), 12433 (2017).
[54] M. Dumont, F. Tuzet, S. Gascoin, G. Picard, S. Kutuzov, M. Lafaysse, B. Cluzet, R. Nheili, T. H. Painter, Journal of Geophysical Research Earth Surface **125**(9), e2020JF005641 (2020).
[55] R. R. Draxler, P. Ginoux, A. F. Stein, J. Geophys. Res. **115**(D16), 2009JD013167 (2010).
[56] P. Achakulwisut, L. Shen, L. J. Mickley, Journal of Geophysical Research Atmospheres **122**(22), 12449 (2017).
[57] A. J. Parolari, D. Li, E. Bou-Zeid, G. G. Katul, S. Assouline, Environmental Research Letters **11**(11), 114013 (2016).
[58] Y. Shao, M. Klose, K. Wyrwoll, Journal of Geophysical Research Atmospheres **118**(19), 11107 (2013).

[59] B. Pu, P. Ginoux, Scientific Reports **7**(1), 5553 (2017).
[60] P. Formenti, L. Schütz, Y. Balkanski, K. Desboeufs, M. Ebert, K. Kandler, A. Petzold, D. Scheuvens, S. Weinbruch, D. Zhang, Atmos. Chem. Phys. **11**(16), 8231 (2011).
[61] J. Wang, M. J. Cubison, A. C. Aiken, J. L. Jimenez, D. R. Collins, Atmos. Chem. Phys. **10**(15), 7267 (2010).
[62] C. R. Hoyle, V. Pinti, A. Welti, B. Zobrist, C. Marcolli, B. Luo, Á. Höskuldsson, H. B. Mattsson, O. Stetzer, T. Thorsteinsson, G. Larsen, T. Peter, Atmos. Chem. Phys. **11**(18), 9911 (2011).
[63] M. Shrivastava, M. O. Andreae, P. Artaxo, H. M. J. Barbosa, L. K. Berg, J. Brito, J. Ching, R. C. Easter, J. Fan, J. D. Fast, Z. Feng, J. D. Fuentes, M. Glasius, A. H. Goldstein, E. Gomes Alves, H. Gomes, D. Gu, A. Guenther, S. H. Jathar, S. Kim, Y. Liu, S. Lou, S. T. Martin, V. F. McNeill, A. Medeiros, S. S. de Sá, J. E. Shilling, S. R. Springston, R. A. F. Souza, J. A. Thornton, G. Isaacman-VanWertz, L. D. Yee, R. Ynoue, R. A. Zaveri, A. Zelenyuk, C. Zhao, Nat. Commun. **10**(1,) 1046 (2019).
[64] X. Dong, J. S. Fu, K. Huang, N.-H. Lin, S.-H. Wang, C.-E. Yang, Sci. Rep. **8**(1), 8962 (2018).
[65] K. Huang, J. S. Fu, N. Lin, S. Wang, X. Dong, G. Wang, Journal of Geophysical Research Atmospheres **124**(16), 9464 (2019).
[66] X. Wu, H. Yang, D. W. Waugh, C. Orbe, S. Tilmes, J.-F. Lamarque, Atmos. Chem. Phys. **18**(10), 7439 (2018).
[67] K. Klingmüller, J. Lelieveld, V. A. Karydis, G. L. Stenchikov, Atmos. Chem. Phys. **19**(11), 7397 (2019).
[68] J. K. Ridley, M. A. Ringer, R. M. Sheward, Climatic Change **139**(2), 325 (2016).
[69] J. F. Kok, D. S. Ward, N. M. Mahowald, A. T. Evan, Nat. Commun. **9**(1), 241 (2018).
[70] B. Sun, P. Yang, G. W. Kattawar, M. I. Mishchenko, Opt. Lett. **42**(23), 5026 (2017).
[71] A. V. Bakian, R. S. Huber, H. Coon, D. Gray, P. Wilson, W. M. McMahon, P. F. Renshaw, American Journal of Epidemiology **181**(5), 295 (2015).
[72] W. Hu, M. Hi, W. Hu, J. Zheng, C. Chen, Y. Wu, S. Guo, Atmos. Chem. Phys. **17**(16), 9979 (2017).
[73] A. Tsikerdekis, P. Zanis, A. L. Steiner, F. Solmon, V. Amiridis, E. Marinou, E. Katragkou, T. Karacostas, G. Foret, Atmos. Chem. Phys. **17**(2), 769 (2017).
[74] P. F. Caffrey, M. D. Fromm, G. P. Kablick, Journal of Geophysical Research Atmospheres **123**(13), 6880 (2018).
[75] B. Pu, P. Ginoux, S. B. Kapnick, X. Yang, Geophysical Research Letters **46**(15), 9163 (2019).
[76] D. Kim, M. Chin, H. Yu, T. Diehl, Q. Tan, R. A. Kahn, K. Tsigaridis, S. E. Bauer, T. Takemura, L. Pozzoli, N. Bellouin, M. Schulz, S. Peyridieu, A. Chédin, Brigitte Koffi, Journal of Geophysical Research Atmospheres **119**(10), 6259 (2014).
[77] S. Dey, S. N. Tripathi, R. P. Singh, B. N. Holben, J. Geophys. Res. **109**(D20), 2004JD004924 (2004).
[78] H. Yu, M. Chin, T. Yuan, H. Bian, L. A. Remer, J. M. Prospero, A. Omar, D. Winker, Y. Yang, Y. Zhang, Z. Zhang, C. Zhao, Geophysical Research Letters **42**(6), 1984 (2015).
[79] L. Liu, M. I. Mishchenko, W. Patrick Arnott, Journal of Quantitative Spectroscopy and Radiative Transfer **109**(15), 2656 (2008).
[80] M. R. Vuolo, H. Chepfer, L. Menut, G. Cesana, J. Geophys. Res. **114**(D9), 2008JD011219 (2009).
[81] Ali. A. Attiya, B. G. Jones, SN Appl. Sci. **2**(5), 845 (2020).

*Corresponding author: anca@inoe.ro